



## OPEN ACCESS

## EDITED BY

Zhigang Li,  
Sun Yat-sen University, Zhuhai Campus,  
China

## REVIEWED BY

Gege Hui,  
Sun Yat-sen University, China  
Webster Mohriak,  
Rio de Janeiro State University, Brazil

## \*CORRESPONDENCE

Jialing Zhang,  
zjl\_9900@163.com  
Mingju Xu,  
11738013@zju.edu.cn

## SPECIALTY SECTION

This article was submitted  
to Marine Geoscience,  
a section of the journal  
Frontiers in Earth Science

RECEIVED 10 August 2022

ACCEPTED 03 October 2022

PUBLISHED 05 January 2023

## CITATION

Wu Z, Zhang J, Xu M and Li H (2023),  
Magnetic anomaly lineations in the  
Northeastern South China Sea and their  
implications for initial  
seafloor spreading.  
*Front. Earth Sci.* 10:1015856.  
doi: 10.3389/feart.2022.1015856

## COPYRIGHT

© 2023 Wu, Zhang, Xu and Li. This is an  
open-access article distributed under  
the terms of the [Creative Commons  
Attribution License \(CC BY\)](https://creativecommons.org/licenses/by/4.0/). The use,  
distribution or reproduction in other  
forums is permitted, provided the  
original author(s) and the copyright  
owner(s) are credited and that the  
original publication in this journal is  
cited, in accordance with accepted  
academic practice. No use, distribution  
or reproduction is permitted which does  
not comply with these terms.

# Magnetic anomaly lineations in the Northeastern South China Sea and their implications for initial seafloor spreading

Zhaocai Wu<sup>1</sup>, Jialing Zhang<sup>1,2\*</sup>, Mingju Xu<sup>1\*</sup> and Hailong Li<sup>3</sup>

<sup>1</sup>Key Laboratory of Submarine Geoscience, Second Institute of Oceanography, Ministry of Natural Resources, Hangzhou, China, <sup>2</sup>Ocean College, Zhejiang University, Zhoushan, China, <sup>3</sup>The Key Laboratory of Gas Hydrate, Ministry of Natural Resources, Qingdao Institute of Marine Geology, Qingdao, China

Ridge jumps occurred during the spreading process of the South China Sea. Recent research on the lower crustal reflectors event on seismic profiles found at least two southward ridge jumps, but only one has been confirmed by geomagnetic data. Based on magnetic anomalies in the northern South China Sea and the “two ridge jumps” model, this study identified that an early ridge jump occurred at anomaly C10n (28.3 Ma), with a southward jump of 20 km. According to the magnetic lineation distribution in the northern South China Sea, initial spreading was dominated by local punctiform break-up and the oldest anomaly, C12n (~30.8 Ma), appeared at two turns of COB. In the IODP Expedition 367&368 drilling area, the continuity of magnetic anomalies from Ridge A to Ridge C was enhanced gradually, representing the transition from local magmatism before the final crustal break-up to a stable igneous oceanic crust. The earliest seafloor spreading magnetic lineation in the Northwestern Sub-basin is C12n (~30.8 Ma) and the magnetic lineation corresponding to the fossil spreading ridge is C10r (~29 Ma). The average half-spreading rate was ~27.2 mm/yr. The opening of the Northwestern Sub-basin appears to have been rotated around a fixed point at the west, with a fault at the eastern end formed by the trajectory of the conjugate point moving during seafloor spreading.

## KEYWORDS

Northeastern SCS, magnetic anomaly lineations, initial seafloor spreading, two ridge jumps, 28.3 Ma

## Introduction

In contrast to the stable seafloor spreading ridge in the Atlantic and the symmetric free drifts of the plates on both sides, the initial spreading of the South China Sea (SCS) was asymmetric. The north continental margin (South China Block) was relatively stable. However, the southern continental margin drifted southward (Figure 1). This implies that the spreading ridge of the SCS exhibited continuous southward movement or intermittent southward jumps during seafloor spreading (Taylor and Hayes, 1983; Briais et al., 1993).

The magnetic lineation model of one ridge jump has been verified using recent geomagnetic data (Li et al., 2014). In previous magnetic lineation models concerning the spreading of the SCS, no reversal of magnetic lineation was present after the ridge jump. On the other hand, the one-jump model is insufficient to explain the asymmetric spreading of the SCS.

A recent study on the lower crustal reflectors based on the multi-channel seismic (MCS) profiles found that at least two southward ridge jumps occurred during the opening of the SCS. The second ridge jump event explained in this new model is consistent with the interpretation of magnetic lineation (Briaies et al., 1993; Li et al., 2014). However, the first ridge jump event has not yet been recognized in terms of magnetic anomalies.

In this study, the age of the first ridge jump event was recognized by reorganizing high-resolution magnetic anomalies in the northern SCS and combining the “two ridge jumps” model interpreted by seismic profiles. On this basis, the magnetic lineation features of initial seafloor spreading in the northern SCS were determined.

## Geological background

The SCS is located at the intersection of the Eurasian Plate, Indo-Australian Plate, and the Philippine Plate. The SCS has experienced continental margin rifting, continental crust break-up, and seafloor spreading since the Cenozoic (Figure 1). Studying the spreading history and tectonic evolution of the SCS is important for understanding the Cenozoic structure in East Asia and surrounding areas (Wang et al., 2019; Li et al., 2021).

In early studies on the seafloor spreading of the SCS, a geophysical survey including the reflection seismic and geomagnetic field data was carried out towards the end of the 1960s. An approximately E-W trending magnetic anomaly lineation of unknown age was discovered, for the first time, in the Eastern sub-basin (Emery and Ben-Avraham, 1972; Ben-Avraham and Uyeda, 1973). However, this finding was uncertain due to limitations in terms of data precision. Subsequently, Briaies et al. (1993) organized all available data regarding magnetic anomalies in the SCS by 1990, and proposed the most detailed results regarding the spreading history of the SCS to date. They pointed out that the ridge jumped southward during 25–23 Ma, and the trend changed from EW to NE-SW.

Barckhausen et al. (2014) proposed that the initial spreading age of the eastern basin was 32 Ma, based on the profiling analysis results of magnetic anomalies in the SCS basin and the southward ridge jump at 25 Ma. Further, the Southwestern sub-basin began to open, and both stopped expanding simultaneously at 20.5 Ma. This phenomenon has led to significant controversy in the research community (Barckhausen, et al., 2015; Chang, et al., 2015). The approximately NW-trending Zhongnan Fault, between the Eastern sub-basin and Southwestern sub-basin,

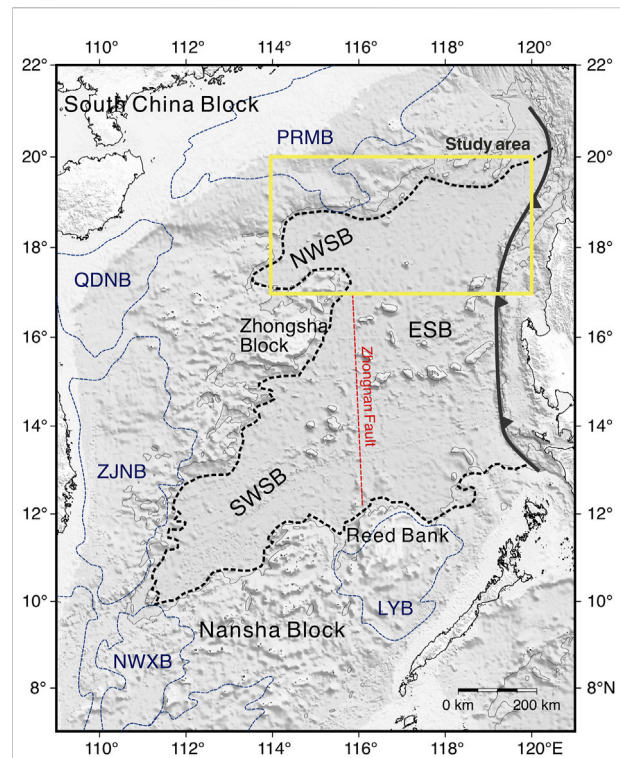


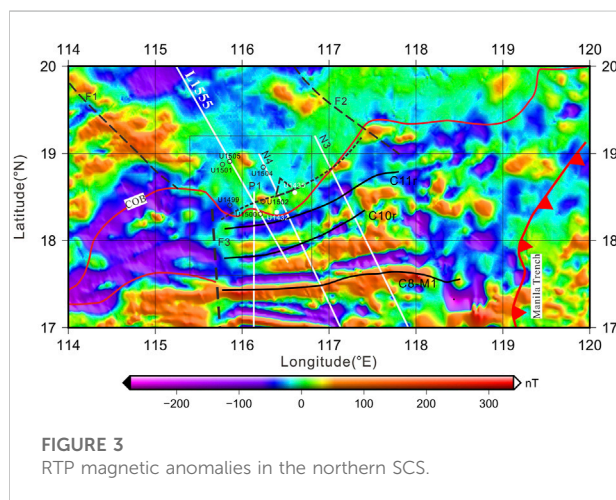
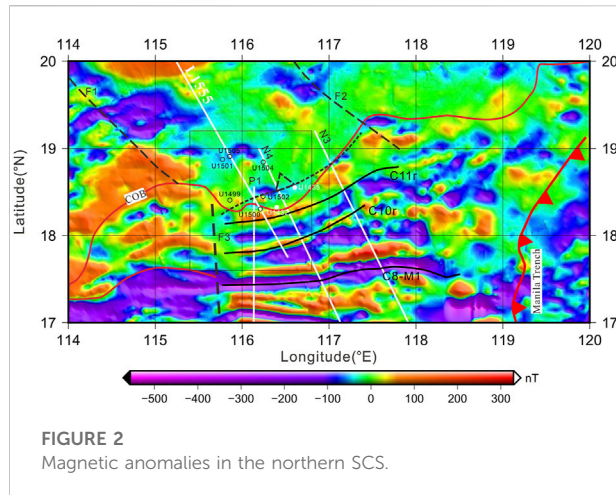
**FIGURE 1**

Morphological features and major tectonic of the SCS. The blue dashed lines are the boundary of the basin, and the thick black dashed line is the COB bounded by the 10 km crustal thickness (Wu et al., 2017). NWSB: Northwestern sub-basin, ESB: Eastern sub-basin, SWSB: Southwestern sub-basin, PRMB: Pearl River Mouth Basin, QDNB: Qiongdongnan Basin, ZJNB: Zhongjiannan Basin, NWSB: Nanweixi Basin, LYB: Liyue Basin.

has also been investigated, and the Liyue Bank is considered to be conjugated with the Zhongsha Block (Barckhausen et al., 2014).

Based on the latest deep-tow magnetic anomaly profiles and IODP349 drilling data, Li et al. (2014) determined that a southward ridge jump of 20 km occurred around 23.6 Ma in the East sub-basin. Furthermore, seafloor spreading propagated to the Southwest sub-basin during 23.6 Ma–21.6 Ma. The terminal age of seafloor spreading is 15 Ma in the Eastern sub-basin and 16 Ma in the Southwestern sub-basin. In their interpretation, an approximately NS-trending Zhongnan Fault was introduced separately into the Eastern sub-basin and Southwestern sub-basin. The extinct spreading centre before the jump was about 170 km away from the north COB and 180 km away from the current extinct spreading centre in the south.

A recent study on the lower crustal reflector (LCR) event on seismic profiles N3 and N4 of the northern SCS found two groups of conjugate LCR structures, and suggested that these conjugate events were related to episodic ridge jumps, which occurred around 27 Ma and 23.6 Ma, according to the calculations of the



asymmetric accretion offset (Ding et al., 2018). The process of the second jump, as determined based on seismic profiles, was consistent with the results of the geomagnetic interpretation model (Li et al., 2014). However, the first ridge jump has not been verified by the magnetic lineation model. Further, to the best of our knowledge, no existing magnetic lineation model has explained the age reversal of the ocean crust after the ridge jump.

## Data and methods

The magnetic anomaly data used in this study was mainly shipboard magnetic data accumulated in the offshore regions of China over several years. The mean square error was smaller than 4 nT and the data grid spacing was 1 arc-minute (Wu et al., 2019). The magnetic anomalies are shown in Figure 2. Since the study area is of a low magnetic latitude, low-latitude reduction to the pole (RTP) was performed using the iterative energy-balancing method, which not only ensures the recovery of abnormalities but also

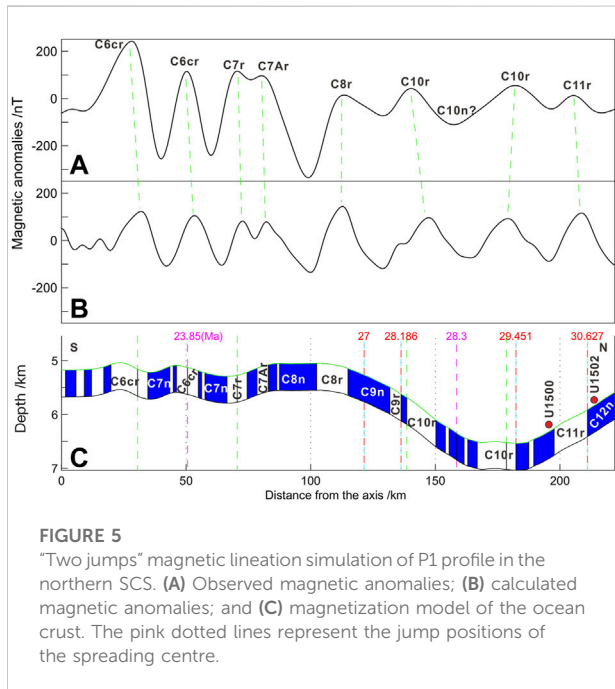
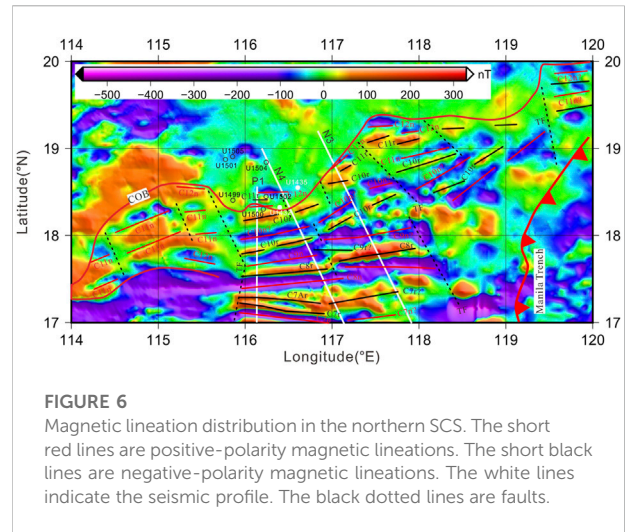
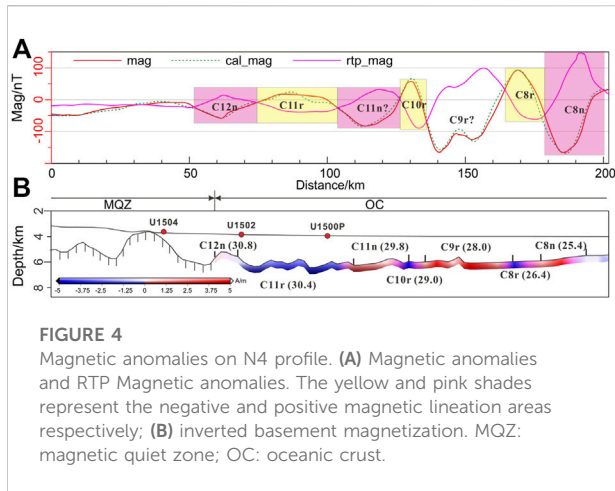
guarantees a robust anomaly amplitude (Li, 2008). The obtained RTP magnetic anomalies are shown in Figure 3. It can be seen that the previously recognised negative magnetic anomaly lineations (C11r and C10r) correspond to the positive magnetic anomaly belt before the RTP. The converse was true for the positive magnetic anomaly lineation C8, which corresponded to the negative magnetic anomaly belt before the RTP and the positive magnetic anomaly belt after the RTP. This completely agrees with the effect of magnetic anomalies under low-latitude and approximately horizontal magnetisation. Thus, the reliability of the RTP magnetic anomalies was confirmed.

The magnetic lineation fitting of profiles was conducted using MODMAG (Mendel et al., 2005), which has been extensively applied in the field of ocean magnetic lineation analysis (Li et al., 2014; Dumais et al., 2020).

## Results

The magnetic anomalies and RTP magnetic anomalies in the northern SCS are shown in Figure 2 and Figure 3, respectively. The continent-ocean boundary (COB), in red, was determined according to the 10 km thickness of the crust, which was obtained by gravity inversion (Wu et al., 2017). This is consistent with the position determined by the seismic profile (Piao et al., 2022). The F1 and F2 Faults are the Yangjiang-Yitong East Fault and Huidong-Beiweitan Fault. Both were deduced to be important base faults in the Mesozoic (Chen et al., 2005) and the Mesozoic subduction accretion zone (Zhou and Yao, 2009) (black dotted lines with arrows in Figure 2 and Figure 3). F3 is the north extension of the Zhongnan Fault, which is a transform fault identified by previous researchers (Taylor and Hayes, 1980, 1983; Larsen, et al., 2018). The F1 fault connected with the F3 fault after extending southward at the border between the Eastern sub-basin and the Northwestern sub-basin. The three magnetic lineations in black solid lines originated from the data of Li et al. (2014).

The two groups of symmetric LCR structures on the seismic profile N4 were assumed to correspond to the two southward ridge jumps (Ding et al., 2018). Comparing the magnetic anomalies on N4 profile, it is clear that the previously identified magnetic lineation (Li et al., 2014) fell within the positive and negative intersection range of magnetic anomalies and RTP magnetic anomalies, which conformed to the low-latitude sub-horizontal magnetic anomaly features (Figure 4A). The inversion results of the magnetization on the N4 profile is shown in Figure 4B. The boundaries between positive and negative magnetisation are expressed as black lines. There were variations in magnetization in each interval of the positive and negative magnetizations. The negative magnetization intervals are expressed as a blue gradient, and the positive magnetization intervals are expressed as a red gradient. It is clear that these positive and negative magnetization intervals were consistent with those determined according to the magnetic anomalies in Figure 4A. However, the amplitude of C9r



decreased significantly and the lineation features were submerged in the negative magnetic anomaly lineation produced by C10r and C8r at the two sides (Figure 4A). C9r has no negative magnetization, but a reduction in magnetization intensity in the middle. According to the magnetic lineation fitting on the deep-tow magnetic anomaly profile de12 (Li et al., 2014), the fitted positive magnetic anomaly signals corresponding to C9r were not observed. In the plane graph of magnetic anomalies (Figure 2), the weak magnetic anomalies that were approximately EW trending were among the background field of the strong negative anomalies, without signs of eastward extension. However, they were integrated with the high-amplitude magnetic anomalies toward the west. These magnetic anomalies exhibited significantly

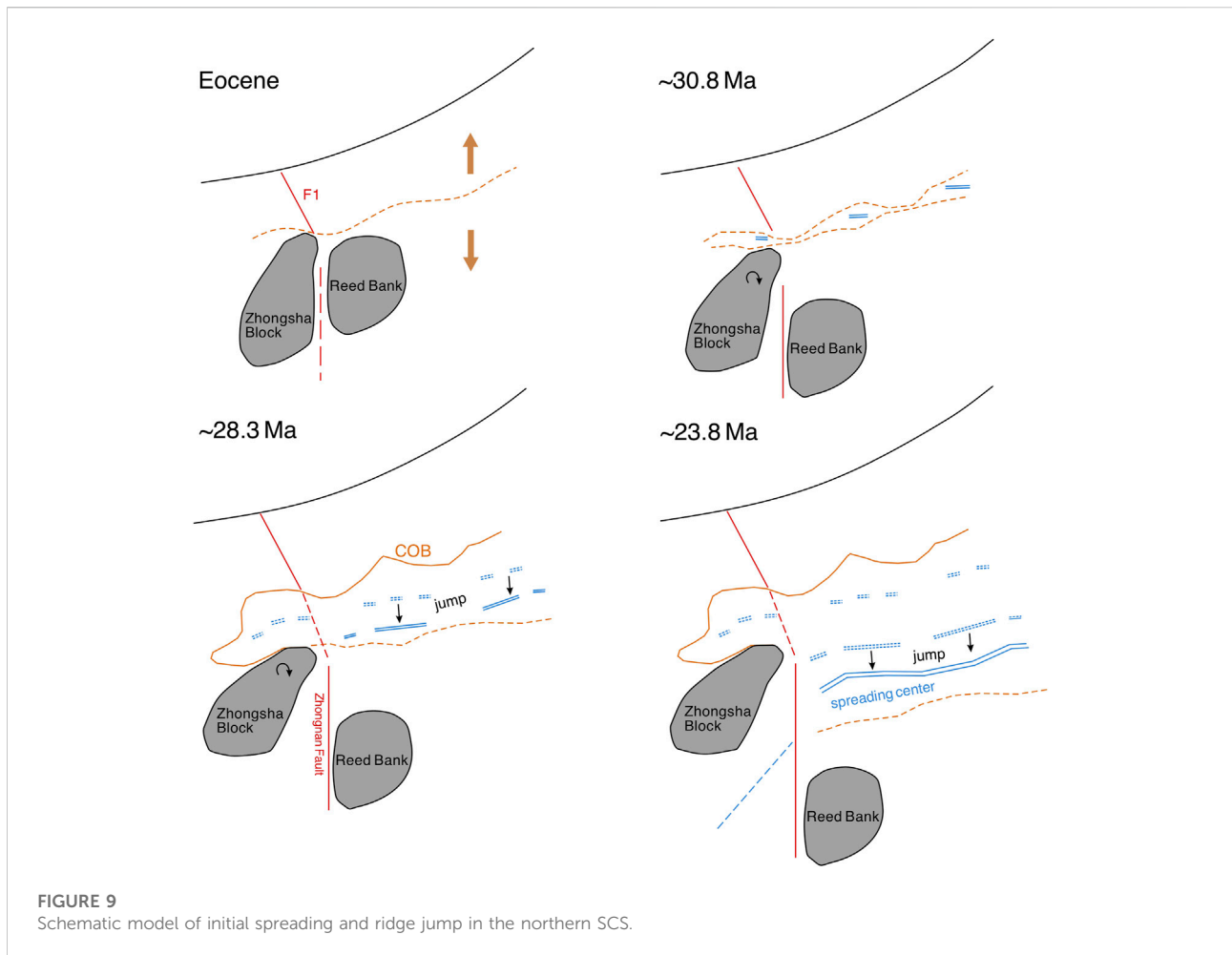
different characteristics for the magnetic lineations at the north and south sides. A group of LCR structures exist in this region (Ding et al., 2018), indicating that this may be the location of the first ridge jump.

Therefore, one approximately NS-trending profile (P1 in Figure 2 and Figure 3) was chosen in the northern SCS for the magnetic lineation simulation according to the "two jumps" spreading model. The magnetic lineation that the profile ran through had relatively good continuity and was able to avoid the confounding effects of any breakage in the magnetic anomalies. The magnetic lineation fitting was completed using MODMAG (Mendel et al., 2005). The calculation parameters were selected in reference to the de12 deep-tow magnetic profile (Li et al., 2014). The simulation results are shown in Figure 5.

The negative magnetic anomaly region between the two magnetic lineations of C10r is the position of the first ridge jump (Figure 5). The corresponding magnetic lineation jumped 20 km southward near C10n at 28.3 Ma. The second ridge jump was near C6cr on the south side, where it jumped 20 km southward at 23.85 Ma. In the "two jumps" model, the time and position of the second jump are consistent with those in previous research. However, the positive magnetic anomalies of C9r were masked by anomalies at the two sides due to the first ridge jump at 28.3 Ma, which is in agreement with observed magnetic anomalies. In other words, C11r could move continuously toward the north, reaching the north side of U1500, and U1502 was over magnetic anomaly C12n (Figure 5).

The "two ridge jumps" model of P1 fitting conforms to the observation of magnetic anomalies and seismic profiles. On this basis, the distribution of magnetic lineations in the northern SCS was tracked (Figure 6). The results showed that, in the initial spreading stage of the SCS, the Eastern sub-basin and the Northwestern sub-basin opened almost simultaneously. The Northwestern sub-basin stopped spreading at C10r (~29.0 Ma). Subsequently, the spreading centre of the Eastern sub-basin





Ridge A, as expressed in the acoustic basement, extended from Sites U1499 to U1502 along the COB. However, the magnetic anomalies of U1499 and U1502 had significantly different characteristics. The former was a low-magnetic anomaly region, indicating the absence of any strong magnetic source. Moreover, this is consistent with the result that breccia was encountered during the drilling of the basement. Borehole U1502 was drilled on the locally high-magnetic anomalies, and the encountered basement was basalt with a strong hydrothermal alteration (Larsen et al., 2018). Hence, the locally high magnetic anomalies differed from the OMH at Sites U1501 and U1505. According to the trend of the magnetic anomalies, Ridge A could extend eastward to Site U1435 of the IODP349 expedition, and is also an OMH; therefore, they may have the same origin. The continuity of such high magnetic anomalies was unstable. For example, there were locally low-magnetic anomalies between Sites U1499 and U1502, as well as between Sites U1502 and U1435. This might be related to the local magmatic activity before the final crust break-up. According to the tracking results of the “two ridge jumps” model, the magnetic anomaly C12n was located at these positions. According to the GPTS2004 geomagnetic time scale

(Ogg and Smith, 2004), the corresponding age was between 30.627 and 31.116 Ma.

Site U1500 drilled Ridge B and penetrated pillow, which corresponded to the magnetic anomaly C11n. Ridge B had better continuity than Ridge A and could extend eastward to Site U1432. However, Ridge B is marked by local interruptions when it is extended eastward, indicating that Ridge B is closer to the location of the final crustal break-up than Ridge A.

Ridge C was in the negative lineation of the RTP magnetic anomalies. Similar to C10n, Ridge C corresponded to the first jump position in the “two ridge jumps” model. The east–west continuity of the negative magnetic lineation was extremely developed and could be found in the entire northern SCS along the COB, which was dominated by the stable accretion of igneous oceanic crust.

## Spreading process of the northwestern sub-basin

The Northwestern Sub-basin has narrow spaces. On one hand, magnetic anomaly lineations are rarely sequential. On the other

hand, the morphological characteristics of these magnetic anomaly lineations have different forms than typical oceanic crust, resulting in great differences in the basin age determined according to magnetic lineations. According to the interpretation of the seismic profile, the Northwestern sub-basin has one additional set of Cenozoic sedimentary strata than the Eastern sub-basin. It is speculated that the Northwestern sub-basin is older than the Eastern sub-basin. The sedimentary sequences filling the Northwestern and Eastern sub-basins are comparable in continuity, which is attributed to simultaneous spreading. Three high-resolution seismic profiles that run through the Northwestern sub-basin all suggested that both the Northwestern and Eastern sub-basins began to open simultaneously, and that the basin opening was characterised by a spreading direction from the east to the west (Ding et al., 2009; Cameselle et al., 2015).

According to magnetic anomalies in the Northwestern sub-basin (Figure 2 and Figure 3) and the previous magnetic lineation tracking results. Combining this finding with the recognised age of the magnetic lineations in the IODP drilling area and the RTP magnetic anomaly features in the Northwestern sub-basin, it was concluded that the magnetic lineation at the initial spreading of the Northwestern sub-basin was C12n (~30.8 Ma), and the azimuth angle was about 99°. The location of the initial spreading of the Northwestern sub-basin was thus determined. The symmetric magnetic lineation near the Shuangfeng seamount was C11n (~29.8 Ma), a product of the follow-up westward spreading, with an azimuth angle of about 63°. The magnetic lineation corresponding to the fossil spreading centre was C10r (~29 Ma) (white dotted lines in Figure 8) rather than the Shuangfeng seamount. The distance between the two C12n positions was 98 km, suggesting an average half-spreading rate of about 27.2 mm/yr.

The striking changes in the recognised magnetic lineations are consistent with the boundary forms of the Northwestern sub-basin. The magnetic lineation striking (spreading direction) also changed gradually with changes in the boundary form. In other words, the boundary form controls the local spreading direction. It seems that the spreading process of the Northwestern sub-basin was formed by the rotation of the Zhongsha Block on the south side around a fixed point at the west end. In this way, the Northwestern sub-basin developed from east to west, and the north section of the Zhongnan Fault was formed along the trajectory of the initial break-up conjugation points (points A and B in Figure 8).

Based on the NW trending changes of the north section of the Zhongnan Fault and the form of the Northwestern sub-basin, it is speculated that the Northwestern sub-basin may have formed by gradual “avulsion” from east to west along the pre-existing NW trending Yangjiang-Yitong Fault (F1 in Figure 8) during the earliest spreading of the Eastern sub-basin, rather than experiencing typical spreading. In other words, the crustal break-up occurred from east to west under the extension stress of the region. This also implies that the Zhongsha Block may have experienced a clockwise rotation at about 30 Ma, rather than simply drifting southward, controlling the Northwestern sub-basin formation (Figure 9).

## Conclusion

The characteristics of the magnetic anomalies and the initially spreading magnetic lineation were discussed herein based on a new survey on shipboard magnetic anomalies in the northern SCS. The calculated RTP magnetic anomalies in the lower crust reflector structures found in the seismic profiles were also analysed. Some major conclusions can be drawn, as follows.

- 1) There were two ridge jumps during the initial spreading of the SCS. The spreading centre jumped 20 km southward at 28.3 Ma. The corresponding magnetic lineation was near C10n. The second ridge jump occurred at 23.85 Ma, which was southward another 20 km. The corresponding magnetic lineation was near C6cr.
- 2) The initial spreading of the SCS was controlled by the COB in the northern SCS, which was locally dominated by punctiform break-up. The oldest magnetic anomaly (C12n) occurred at the two turns of the COB.
- 3) Ridge A, in the IODP drilling area, is a locally high-magnetic anomaly with poor continuity; it corresponds to C12n (30.8 Ma). Ridge A is related to the local magmatic activity before the final break-up. Ridge B corresponds to C11n, and its continuity is relatively good; it is located at the onset of the oceanic crust. Ridge C is close to C10n and corresponds to the first ridge jump. The magnetic lineation exhibits stable continuity from east to west, which can be seen in the entire northern SCS along the COB. In summary, Ridge C has become normal oceanic crust for stable spreading.
- 4) C12n is the oldest magnetic lineation in the Northwestern sub-basin (~30.8 Ma). C11n is the symmetric magnetic lineation near the Shuangfeng seamount (~29.8 Ma). C10r is the magnetic lineation corresponding to the fossil spreading centre (~29 Ma), with an average half-expansion rate of approximately 27.2 mm/yr. The Northwestern sub-basin seems to have opened from east to west, with rotation around a fixed point at the west end. Moreover, the north section of the Zhongnan Fault is formed along the trajectory of the conjugation break-up point during seafloor spreading.

## Data availability statement

The data analyzed in this study is subject to the following licenses/restrictions: Institutions are not allowed to publish data. Requests to access these datasets should be directed to ZW, wuzc@sio.org.cn.

## Author contributions

ZW: Conceived this research, Writing—original draft, Funding support, JZ: Edited this article and discussed the

results and interpretation, MX: Data Processing and Methodology, editing, HL: Funding support and review.

## Funding

This research is supported by the National Natural Science Foundation of China (grant numbers 42076078 and 42006068).

## Acknowledgments

We would like to thank the editor and reviewers for their critical and constructive comments. The magnetic lineation fitting was completed using MODMAG (Mendel, et al., 2005).

## References

- Barckhausen, U., Engels, M., Franke, D., Ladage, S., and Pubellier, M. (2014). Evolution of the South China Sea: Revised ages for breakup and seafloor spreading. *Mar. Pet. Geol.* 58, 599–611. doi:10.1016/j.marpetgeo.2014.02.022
- Barckhausen, U., Engels, M., Franke, D., Ladage, S., and Pubellier, M. (2015). Reply to Chang et al., 2014, Evolution of the South China Sea: Revised ages for breakup and seafloor spreading. *Mar. Pet. Geol.* 59, 679–681. doi:10.1016/j.marpetgeo.2014.09.002
- Ben-Avraham, Z., and Uyeda, S. (1973). The evolution of the China Basin and the mesozoic paleogeography of Borneo. *Earth Planet. Sci. Lett.* 18, 365–376. doi:10.1016/0012-821X(73)90077-0
- Bonatti, E. (1985). Punctiform initiation of seafloor spreading in the Red Sea during transition from a continental to an oceanic rift. *Nature* 316, 33–37. doi:10.1038/316033a0
- Briais, A., Patriat, P., and Tapponnier, P. (1993). Updated interpretation of magnetic anomalies and seafloor spreading stages in the south China Sea: Implications for the tertiary tectonics of southeast Asia. *J. Geophys. Res.* 98, 6299–6328. doi:10.1029/92jb02280
- Cameselle, A. L., Ranero, C. R., Franke, D., and Barckhausen, U. (2015). The continent-Ocean transition on the Northwestern South China Sea. *Basin Res.* 29, 73–95. doi:10.1111/bre.12137
- Chang, J. H., Hsu, H. H., Liu, C. S., Lee, T. Y., Chiu, S. D., Su, C. C., et al. (2015). Seismic sequence stratigraphic analysis of the carbonate platform, north offshore Taiping Island, Dangerous Grounds, South China Sea. *Tectonophysics* 702, 70–81. doi:10.1016/j.tecto.2015.12.010
- Chen, H. Z., Wu, X. J., Zhou, D., Wang, W. Y., and Hao, H. Z. (2005). Mesozoic faults in zhujiang River Mouth basin and their geodynamic background. *J. Trop. Oceanogr.* 24, 52–61.
- Ding, W., Sun, Z., Dadd, K., Fang, Y., and Li, J. (2018). Structures within the oceanic crust of the central South China Sea basin and their implications for oceanic accretionary processes. *Earth Planet. Sci. Lett.* 488, 115–125. doi:10.1016/j.epsl.2018.02.011
- Dumais, M., Gernigon, L., Olesen, O., Johansen, S. E., and Brnner, M. (2021). New interpretation of the spreading evolution of the Knipovich Ridge derived from aeromagnetic data. *Geophys. J. Int.* 224, 1422–1428. doi:10.1093/gji/ggaa527
- Emery, K. O., and Ben-Avraham, Z. (1972). Structure and stratigraphy of China basin. *Am. Assoc. Pet. Geol. Bull.* 56, 839–859. doi:10.1306/819A408E-16C5-11D7-8645000102C1865D
- Larsen, H. C., Mohn, G., Nirrengarten, M., Sun, Z., Stock, J., Jian, Z., et al. (2018). Rapid transition from continental breakup to igneous oceanic crust in the South China Sea. *Nat. Geosci.* 11, 782–789. doi:10.1038/s41561-018-0198-1
- Li, C. F., Xing, X., Jian, L., Sun, Z., Zhu, J., Yao, Y., et al. (2014). Ages and magnetic structures of the South China Sea constrained by deep tow magnetic surveys and

## Conflict of interest

The authors declare that the research was conducted in the absence of any commercial or financial relationships that could be construed as a potential conflict of interest.

## Publisher's note

All claims expressed in this article are solely those of the authors and do not necessarily represent those of their affiliated organizations, or those of the publisher, the editors and the reviewers. Any product that may be evaluated in this article, or claim that may be made by its manufacturer, is not guaranteed or endorsed by the publisher.

IODP Expedition 349. *Geochem. Geophys. Geosyst.* 15, 4958–4983. doi:10.1002/2014GC005567

Li, J., Ding, W., Lin, J., Xu, Y., Kong, F., Li, S., et al. (2021). Dynamic processes of the curved subduction system in southeast Asia: A review and future perspective. *Earth-Science Rev.* 217, 103647. doi:10.1016/j.earscirev.2021.103647

Li, X. (2008). Magnetic reduction-to-the-pole at low latitudes: Observations and considerations. *Lead. Edge* 8, 990–1002. doi:10.1190/1.2967550

Mendel, V., Munsch, M., and Sauter, D. (2005). MODMAG, a MATLAB program to model marine magnetic anomalies. *Comput. Geosci.* 31, 589–597. doi:10.1016/j.cageo.2004.11.007

Ogg, J. G., and Smith, A. G. (2004). *The geomagnetic polarity time scale. A Geologic Time Scale 2004*. Editors F. M. Gradstein, J. G. Ogg, and A. G. Smith (Cambridge: Cambridge University Press), 63–86.

Piao, Q. F., Zhang, B. J., Zhang, R. W., Geng, M. H., and Zhong, G. F. (2022). Continent-ocean transition in the northern South China Sea by high-quality deep reflection seismic data. *Chin. J. Geophys.* 65, 2546–2559. doi:10.6038/cjg2022P0663

Sun, Z., Stock, J., Jian, Z., McIntosh, K., Alvarez-Zarikian, C. A., and Klaus, A. (2016). Expedition 367/368 scientific prospectus: South China Sea rifted margin. *Int. Ocean. Discov. Progr.* doi:10.14379/iodp.sp.367368.2016

Taylor, B., and Hayes, D. E. (1983). "Origin and history of the south China Sea basin," in *The tectonic and geologic evolution of southeast asian seas and islands Part 2, geophysical monograph series*. Editor D. E. Hayes (Washington, DC: AGU), 23–56. doi:10.1029/gm027p0023

Taylor, B., and Hayes, D. E. (1980). "The tectonic evolution of the south China Sea basin," *The tectonic and geologic evolution of southeast asian seas and islands, geophysical monograph series*. Editor D. E. Hayes (Washington, DC: AGU), 89–104. doi:10.1029/gm023p0089

Wang, P., Huang, C., Lin, J., Jian, Z., Sun, Z., and Zhao, M. (2019). The South China Sea is not a mini-atlantic: Plate-edge rifting vs intra-plate rifting. *Natl. Sci. Rev.* 6, 902–913. doi:10.1093/nsr/nwz135

Wu, Z. C., Gao, J. Y., Ding, W. W., Shen, Z. Y., Zhang, T., and Yang, C. G. (2017). The Moho depth of the South China Sea basin from three-dimensional gravity inversion with constraint points and its characteristics. *Chin. J. Geophys.* 60, 368–383. doi:10.1002/cjg2.30053

Wu, Z. C., Gao, J. Y., and Yang, C. G. (2019). "Magnetic anomaly map of southern China seas, 1:3,000,000," in *The marine geological series maps of China Sea*. Editors Z. Y. Wu and Z. H. Wen (Beijing: Science Press).

Zhou, D., and Yao, B. (2009). Tectonics and sedimentary basins of the south China Sea: Challenges and progresses. *J. Earth Sci.* 20, 1–12. doi:10.1007/s12583-009-0001-8